ELSEVIER

Journal of Molecular Catalysis A: Chemical 171 (2001) 123–141

JOURNAL OF MOLECULAR CATALYSIS A: CHEMICAL

www.elsevier.com/locate/molcata

A combined theoretical and experimental study of the effects of residual chlorine on the behavior of Pd/γ-Al_2O_3 catalysts for methane oxidation

G. Tonetto*, M.L. Ferreira, D.E. Damiani

PLAPIQUI-(UNS-CONICET), Camino La Carrindanga Km, 7-CC 717, 8000 Bahía Blanca-R, Argentina

Received 12 September 2000; accepted 18 January 2001

Abstract

Studies of the methane oxidation on Pd/γ-Al_2O_3 catalysts with and without chloride were made. The reaction was investigated at temperatures in the range 20–500°C using stoichiometric reactant mixture. Dissociation of methane and oxygen and desorption of carbon dioxide and water on Pd catalysts have been investigated using a Molecular Orbital approach of the Extended Hückel type, including repulsion terms.

Keywords: Extended Hückel molecular orbital (EHMO) method; Pd supported catalyst

1. Introduction

The catalytic combustion of hydrocarbons is becoming of increasing importance both in the production of energy and in gaseous emission control. Catalysts able to perform the combustion reaction are alumina-supported noble metals. In the case of complete oxidation of methane, palladium is the most attractive metal because of its high activity and relatively low cost.

Some papers on methane oxidation reported that chlorine containing precursor salts produce catalysts inferior in performance to others made without chloride [1,2]. Simone et al. [3] suggested that the reversible poisoning may be occurring by the following means: (a) blocking of PdO actives sites by chloride thereby decreasing accessibility of reactant gas to the catalytic site, and/or (b) chemical interaction of chloride with the catalytically active PdO species resulting in $Pd_xO_yCl_z$ complexes, which are less active. Shen et al. [4] reported a bridged structure of chlorine containing palladium catalysts. Marecot et al. [5] investigated the oxidation of propane and propene on palladium and platinum supported catalysts. They found that catalysts prepared from chlorine containing precursor salts, are poisoned by chlorine whatever the particle size and this poisoning effect is more detrimental under oxidizing conditions. After successive reaction cycles, this poisoning effect disappears as consequence of the removal of chlorine from the catalyst surface by water produced during propane and propene combustion. Poisoning effects of chloride are explained by a decreased active surface under consideration consequence of the chemical interaction of the halogen with the catalyst surface. Similar results are presented by Cant et al. [6] for the oxidation of hydrocarbons. Cullis and Willatt [7] suggest that the halogen would be adsorbed on the sites normally necessary for the adsorption and activation of oxygen. Lieske et al. [8] and Barbier et al.

* Corresponding author.

1381-1169/01/$ – see front matter
PII: S1381-1169(01)00078-4

[9] consider the formation of metal oxide-chloride species which are more stable and less reactive than oxygen species. There is agreement about the idea that chlorine is removed more easily under reducing condition whereas oxidative treatments are ineffective [1,3,5,6,10]. Peri and Lund [11] reported that Pd catalysts generally show an induction period followed by an activation period. The first one is associated to the presence of chlorine. The higher the content of chlorine, the longer the induction period. The activation period is probably not related to the presence of chlorine residues. It is important also the place where chlorine resides. Rodríguez Cárdenas and Damiani [12] observed a distortion of the TPR peak belonging to the Pd hydride that was associated to the presence of chlorine nearby the metal or in contact with it. XPS studies on supported Pt catalysts indicate two kinds of chlorine, one is associated with the metal and can be easily removed, while the other is associated with the support and it is difficult to remove [13]. A distinction between chlorine associated with metal and with the support has also been noted for supported Ru [14].

The objective of this work is to examine the effects of chlorine from the precursor salts on the activity of catalysts. In order to gain a better understanding of the reaction, dissociation of methane and oxygen and desorption of carbon dioxide and water on Pd catalysts with and without chlorine have been investigated using Molecular Orbital approach of the Extended Hückel type. Experimental results about methane total oxidation reaction and catalysts characterization are presented and discussed.

2. Experimental

2.1. Catalysts preparation

The Pd/Al_2O_3 catalyst prepared from $Pd(C_5H_7O_2)_2$ is referred to as p1 and the catalyst derived from $Pd(NH_3)_4Cl_2{\cdot}H_2O$ is called p2.

The p1 sample was prepared by impregnation of the support with a solution of $Pd(C_5H_7O_2)_2$ (Alfa) in toluene (Merck). The support material was γ-Al_2O_3 (Condea, Puralox, 148 m^2/g). After impregnation the catalyst was dried in Ar at 150°C for 2 h and then calcined in chromatographic air at 500°C during 2 h.

The p2 catalyst was prepared by impregnation of the support with $Pd(NH_3)_4Cl_2{\cdot}H_2O$ (Spex) using the incipient-wetness method. The support used was γ-Al_2O_3 (Rhone-Poulenc) with BET area of 120 m^2/g and pore volume of 1 cm^3/g. The isoelectric point of the support is 7.5. The pH of precursor solution was 11. It was fixed to 11 with 20% HNO_3 solution. After impregnation the catalyst was dried in Ar at 423 K for 2 h and then calcined in chromatographic air at 500°C during 2 h.

In both catalysts, prior to impregnation the support was dried under N_2 at 150°C for 2 h. The palladium content was determined by Atomic Absorption Spectroscopy.

2.2. H_2 chemisorption

Hydrogen chemisorption experiments were conducted in a conventional pulse apparatus at atmospheric pressure and room temperature. The samples were oxidized in air at 500°C during 1 h and exposed to a temperature-programmed reduction (TPR) experiment in a gas mixture containing 5%H_2–95%Ar in the temperature interval 25–500°C. After cooling to 25°C temperature in Ar, H_2 pulse were admitted until the sample was saturated.

The fraction of exposed palladium was calculated assuming that one hydrogen atom is adsorbed per surface palladium atom. The average crystallite size based on chemisorption measurements was estimated from the equation $d(\text{nm}) = 112/(\text{percentage of metal exposed})$. This expression assumes spherical particles and a surface atom density of 1.27×10^{19} atoms/m^2 [15].

2.3. TPR experiments

TPR experiments were carried out in an apparatus similar to that described by Robertson et al. [16] to which some changes were introduced [17]. The reducing gas was a mixture (5%H_2–95%Ar) first circulated through an empty 6 mm o.d. Pyrex tube positioned in the furnace (the reference), then it passed through a Molecular Sieve 3A cold trap and, after passing through the reference branch of a thermal conductivity detector (TCD), it went to a 6 mm o.d. Pyrex tube containing the catalyst. After leaving the sample the reducing mixture was passed through a Molecular

Sieve 3A cold trap and the measuring branch of the TCD. The TCD was a flow-through type, microvolume, hot wire Gow Mac cell. Standard methods of gas purification were used. The reference and the sample were held in an oven that could be heated at linear rate of 10°C/min between 0 and 500°C. The temperature of the catalyst bed was measured with a 1/16 ft o.d. stainless steel shield chromel–alumel thermocouple placed in contact with the top of the catalyst bed. The flow rate of the reducing gas was 20 $cm^3\ min^{-1}$.

Fresh samples of catalysts (40 mg) were oxidized in flowing chromatographic air at 300°C for 1 h and purged and cooled in Ar to −50°C, followed by TPR. The cycle was repeated with samples oxidized at 500°C in the same conditions.

2.4. Catalytic activity measurements

The catalysts were tested in a horizontal glass-made packed bed reactor (6 mm o.d.) placed in an electrically heated oven. A temperature controller was used to control the reaction temperature (Omega CN3800), which was measured by means of a shielded J type Omega thermocouple placed in the furnace at the same position that the catalyst bed outside the reactor. The reaction mixture composition was 1% CH_4, 2% O_2 and 97% He. The reaction products were analyzed in a Varian 3700 gas chromatography operating in TCD mode. A silica gel (2 m × 1/8 in)-Molecular Sieve 5A (1 m × 1/8 in) and Porapak N (2 m × 1/8 in) columns operated isothermally at 308 K with He at 20 $cm^3\ min^{-1}$ as carrier gas was used for separation. Chromatographic peaks were integrated by means of a Hewlett-Packard 3390 Å integrator.

Catalytic tests were done on catalyst samples that were exposed to calcination step only. The tests were done in two ways: (1) the catalyst sample is heated in the reaction mixture from 293 to 773 K. Samples of the reaction products are taken at different reaction temperatures or (2) the catalyst sample is heated to 773 K in He flow. Once the final temperature is reached the catalyst is contacted with the reaction mixture during 2 h. After that the catalyst temperature is lowered to 623 K under a He flow. When the new reaction temperature is reached the catalyst is contacted again with the reaction mixture during 2 h. Samples of reaction products are taken regularly. Catalyst weight was adjusted in order to keep constant the weight of Pd in the different experiments. The reaction mixture flow rate was maintained at 20 $cm^3\ min^{-1}$.

2.5. IR studies

Infrared spectra of samples were recorded after reaction. The infrared spectra were recorded on a FTIR 520 Nicolet spectrometer with 4 cm^{-1} resolution and 10 scans. The cell was under air flow and the spectra were recorded at room temperature.

3. Theoretical model

The theoretical studies applied to catalysis may be classified in semi-empirical and ab initio methods. Amongst the formers, an extended Hückel molecular orbital (EHMO) method was selected to perform the quantum mechanical study of the Pd/γ-Al_2O_3 catalytic system.

The EHMO was widely used by Hoffman and coworkers [18–20] to study electronic structure of transition metal complexes and adsorbed molecules, it provides useful qualitative trends in large model system. The electronic structure and derived properties are established from electron equations for the molecular orbitals, approximated by experimental data. In this formalism, the non-diagonal elements of Hamiltonian of the system are proportional to the overlap matrix elements. More recently, in order to improve the traditional Extended Hückel Hamiltonian some corrections were introduced by Chamber et al. [21] and Anderson and Hoffman [22].

The total energy of a selected adsorbed molecule on a palladium cluster is a sumatory of an attractive and a repulsive term and may be represented by the following equation:

$$E_t = \sum_i n_i E_i + \frac{1}{2}\sum_i \sum_{i \neq j} E_{\mathrm{rep}\,(i,j)} \quad (1)$$

The attractive energy is related to the electrons in the valence level i with an occupancy n_i. The repulsion energy is originated between all the possible pairs nucleus i-fixed atom j.

Experimental parameters are necessary for calculations, being the EHMO a semi-empirical method. We have used reported ionization potential obtained from

Table 1
Atomic parameters used for EHMO calculation

Atom	Orbital	Ionization potential (eV)	Orbital exponents
Pd	5s	−7.24	2.19
	5p	−3.68	2.15
	4d	−11.90	5.98, 2.61, 0.55, 0.67
O	2s	−31.60	2.163
	2p	−16.78	2.750
H	1s	−13.60	1.00
C	2s	−15.59	1.5536
	2p	−10.26	1.4508
Cl	35	−26.03	2.356
	3p	−14.20	2.039

spectroscopic data [23]. Since for the level 4p only theoretical data are available in literature, we have taken the data of Hartree–Fock–Slater [24]. Parameters used in this work for palladium, oxygen, hydrogen, chloride and carbon are presented in Table 1.

The program used to calculate the energy of the different adsorbed species was the ICONC, originally developed by Chamber et al. [25], which take into account repulsive terms that are not originally in the EHMO. In the present work, calculations were carried out with a modified version of ICONC. This version has been tested in previous work dealing with the adsorption of metallocenes and Ziegler–Natta catalysts [26,27].

The total energy of adsorbed species was calculated as the difference between the electronic energy of the system when the adsorbed molecule is at a finite distance from the surface and when the molecule is far away from the cluster surface. The geometry optimization was done at 0.1 Å step and due to the approximate nature of extended Hückel like methods the convergence criterion to the energy was set to 0.01 eV.

The dissociation energies shown in Tables are defined as the total energy of dissociated species minus the total energies of adsorbed species. It could be considered as a dissociation energy of adsorbed reactives.

The semi-empirical MO calculations have been performed in the framework of the cluster approximation, that is the adsorption site and its neighborhood was modeled by a portion of the otherwise infinite solid.

4. Modeling of surface palladium structures

The dependence of catalytic activity on the chemical state of palladium gave conflicting results [28–32]. Some active forms of palladium that have been proposed for methane oxidation are highly dispersed palladium oxide particles, chemisorbed oxygen on Pd, a layer of oxide on Pd crystallites and surface reconstruction of palladium oxide under reaction condition.

Taking account of the particles size, we decided to model the metal cluster without considering the support. Our Pd catalysts are light brown when they are oxidized and dark gray when they are reduced. The p1 sample changes its color to dark gray after reaction, showing that reduction takes place (at least partially). The p2 sample was light brown before and after reaction. Because this experimental fact we modeled metallic clusters with different oxidized fractions (film and cluster).

4.1. The surface of Pd (2 0 0)

Since the structure of the surface catalysts is unknown, we used the Pd (2 0 0) plane according to Garbowsky et al. [30]. A cluster with 117 atoms were used to represent the (2 0 0) face: 85 Pd and 32 H (Fig. 1). Hydrogen atoms were used to complete the internal palladium coordination and to avoid the undesirable effect called dangling bonds. The Pd atoms were distributed in three layers of 41, 40 and 4 atoms. The geometry of the bulk fcc crystals was used with cell parameter 3.8 Å and interlayer separation of 2.20 Å based on the theoretical work of Ward et al. [33]. Taking into account previous results [34] we have used unrelaxed surface for all the calculations. This model was identified as Pd(0).

4.2. The surface of Pd (2 0 0) partially oxidized

In consideration of the catalyst color after reaction, we decided to model the surface of Pd (2 0 0) partially oxidized. One hundred and twenty-two atoms were used in the model, 5 O, 32 H and 85 Pd placed in three layers like Fig. 2 shows. This structure was chosen because previous work [30] showed that palladium particles exposing the (2 0 0) planes to the reactants easily form PdO (0 0 1), since both have similar parameters. This model was identified as PdO(cluster)/Pd(0).

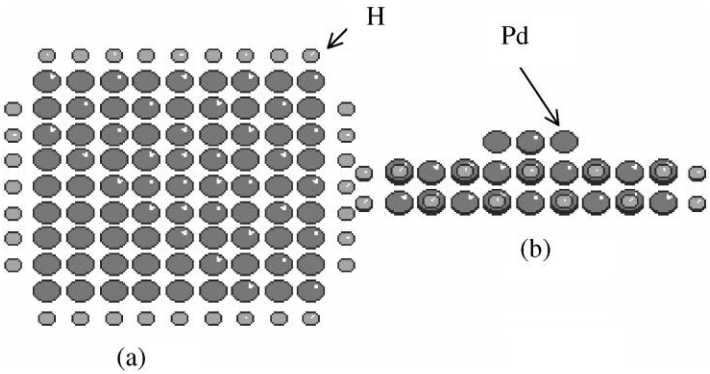

Fig. 1. Pd(0) model: (a) top view; (b) lateral view.

4.3. The surface of PdO (0 0 1)

The model of surface PdO (0 0 1) was constructed with 124 atoms: 32 O, 28 H and 64 Pd, disposed in two layers (Fig. 3). Dangling bonds were satured with hydrogen atoms. This model was identified as PdO(film)/Pd(0).

4.4. The surface of Pd (2 0 0) partially oxidized containing chlorine

A cluster with 124 atoms: 3 Cl, 4 O, 32 H and 85 Pd placed in three layers showed in Fig. 4 was used to model the chlorine containing catalyst. Bridged chlorine structure was introduced in the first layer in order to represent the residual chlorine. Following literature data [35], Pd–Cl distance was set at 2.1 Å. This model was identified as PdO(cluster)-Cl/Pd(0).

4.5. The surface of PdO (0 0 1) containing chlorine

In the same way, Fig. 5 shows the surface of PdO (0 0 1) containing chlorine. 8 Cl, 28 H, 24 O and 64 Pd were used to model the cluster. This model was identified as PdO(film)-Cl/Pd(0).

4.6. Oxygen adsorption and dissociation

Different positions for O_2 adsorption were evaluated:

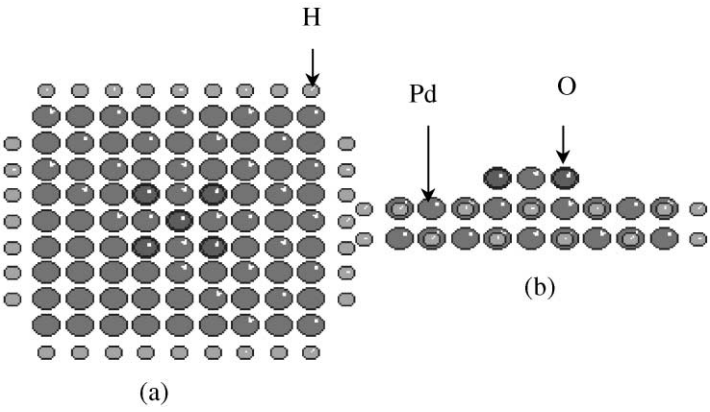

Fig. 2. PdO(cluster)/Pd(0) model: (a) top view; (b) lateral view.

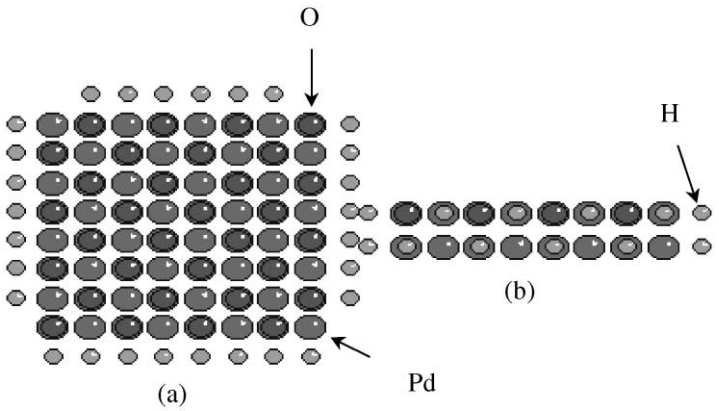

Fig. 3. PdO(film)/Pd(0) model: (a) top view; (b) lateral view.

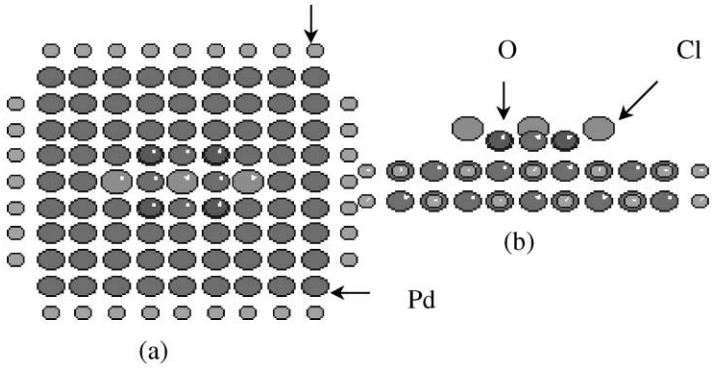

Fig. 4. PdO(cluster)-Cl/Pd(0) model: (a) top view; (b) lateral view.

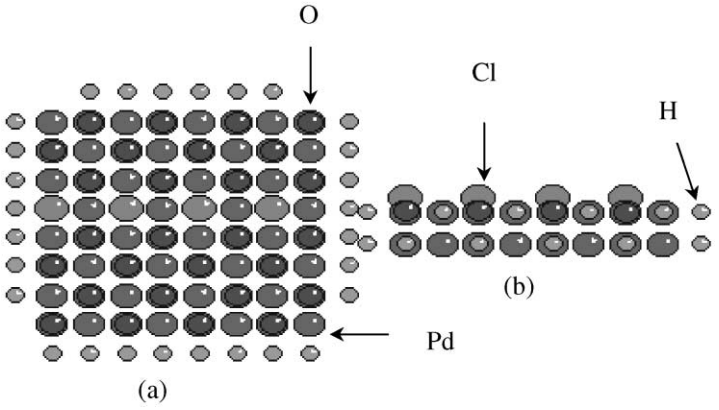

Fig. 5. PdO(film)-Cl/Pd(0) model: (a) top view; (b) lateral view.

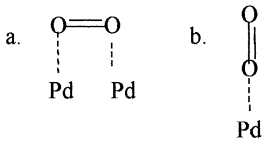

Scheme 1. Model of O_2 adsorption.

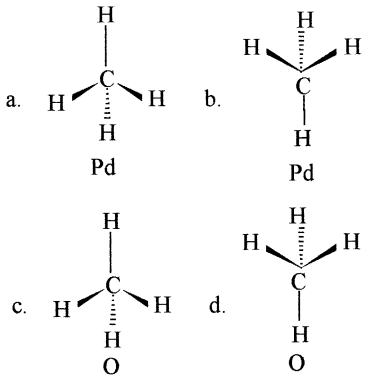

Scheme 2. Model of CH_4 adsorption.

- parallel to the surface plane, each O atom in an "on top" position (Scheme 1a);
- perpendicular to the surface plane, in an "on top" position (Scheme 1b).

Our calculations considered two kinds of adsorbed oxygen species placed at on-top (O_t) and hollow (O_h) sites, which represent the weakly and strongly adsorbed oxygen, respectively.

4.7. Methane adsorption and dissociation

Scheme 2 shows different configurations for methane adsorbed on the clusters:

- one of the tetrahedral axes through the C oriented perpendicularly to the cluster surface, with the C atom closer the Pd or O_h atom;
- one of the tetrahedral axes through the C oriented perpendicularly to the cluster surface, with the H atom closer the Pd or O_h atom.

For the dissociation of CH_4, the CH_3 group maintained the same geometry (≻HCH angle = 109.5° and C–H distance = 1.32 Å) as in the free methane molecule and the abstracted H was positioned on a Pd, O or Cl atom (Scheme 3). The methyl group bonded to Pd or O atom was placed at the distance reported in Table 5. The O_h–H bond was found to be perpendicular to the surfaces [36].

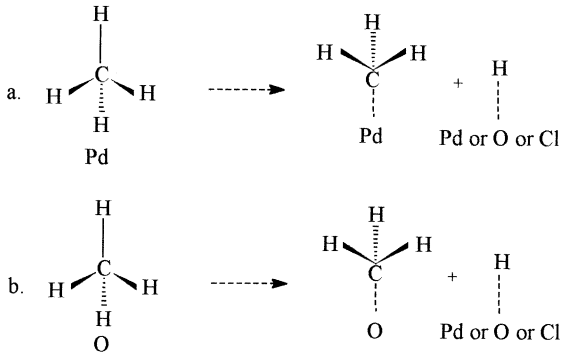

Scheme 3. Model of CH_4 dissociation.

4.8. Chlorine loss

Scheme 4 represents removal of chlorine from the catalyst surface during reaction. H–Cl distance used was 1.2746 Å in all calculations.

4.9. Water adsorption

We consider the H_2O molecule bonded to the Pd atom by the oxygen end and the molecular plane was assumed to be perpendicular to the surface [37]. It maintained the same geometry (≻HOH angle = 104.5° and O–H distance = 0.9575 Å) as in the free water molecule. Water desorption and oxygen vacancy formation also was considered.

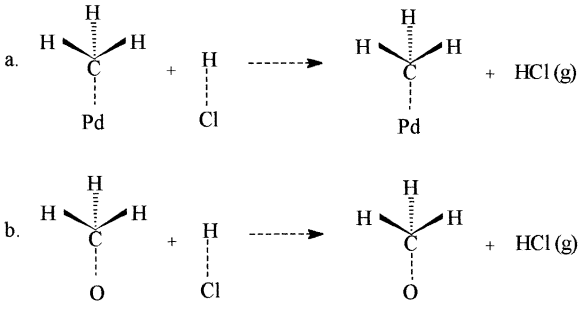

Scheme 4. Removal of chlorine from the catalyst surface during methane combustion.

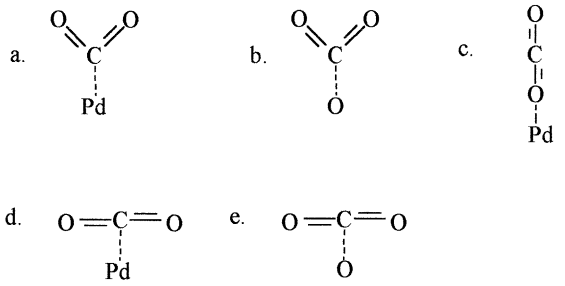

Scheme 5. Model of CO_2 adsorption.

4.10. Carbon dioxide adsorption

The used geometries in the calculation are shown in Scheme 5. C–O distance was 1.27 and 1.31 Å in the carboxylate and carbonate complexes, respectively. In both species we consider C sp^2 (>OCO angle = 120°). For the other structures presented in Scheme 5 the same geometry was maintained (>OCO angle = 180° and O–C distance 1.16 Å) as in the free carbon dioxide molecule.

Numerous investigations of CO_2 adsorbed over metal oxides ([38,39] and references therein) have established the formation of complexes of different types like bicarbonate, monodentate and bidentate carbonate. We choose monodentate species because formation of such bidentate structure would suggest the existence and accessibility of appropriate anion vacancies on the oxide surface.

4.11. Steps of products desorption — reactive adsorption/dissociation

We compared steps of adsorption–dissociation of reactives and products desorption in two possible reaction mechanisms: (a) surface reaction of the Langmuir–Hinshelwood type and (b) a redox mechanism (Mars and van Krevelen), involving the reaction of methane with lattice oxygen of PdO and subsequent reoxidation of palladium formed. The methyl group was bonded to Pd or O atoms. In models containing chlorine, we considered that the abstracted H lies on a Pd or Cl atom as Scheme 6 shows.

5. Results and discussion

5.1. Catalysts preparation

Table 2 presents the catalysts Pd content. As it was mentioned in the Section 2, p1 sample was prepared from $Pd(Acac)_2$ and finally calcined in air. After this treatment, PdO particles are present [40]. Krishnankutty et al. reported that the $Pd(Acac)_2$ precursor is a likely source of carbon which can contaminate the Pd particles. However, calcination and reduction pretreatment (at 300°C) completely cleaned the 0.8 wt.% Pd/SiO_2 catalyst. Lomot et al. [41,42] showed that palladium acetylacetonate binds more strongly to Al_2O_3 than to SiO_2. The organic part of the $Pd(Acac)_2/Al_2O_3$ precursor is subjected to considerable splitting before being stripped off from the support during calcination. An oxidative pretreatment at temperatures higher than 350°C is essential for removing all the carbon from the catalysts surface. Similarly, XPS results [43] reported small amounts of carbonaceous compounds in

Table 2
Characterization of Pd/γ-Al_2O_3 catalysts

Catalyst	Pd loading (wt.%)	H/Pd (298 K)	d (nm)[a]
p1	0.82	0.36	3.1
p2	1.06	0.15	7.5

[a] Calculated from H_2 chemisorption data.

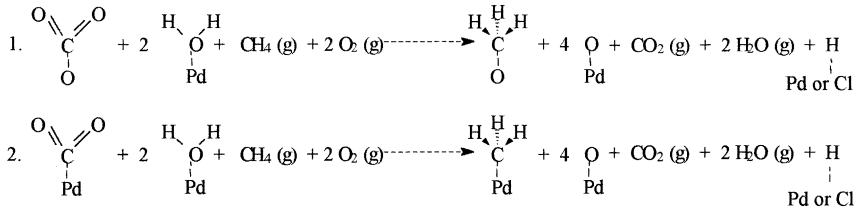

Scheme 6. Products desorption — reactive adsorption.

Pd/SiO_2 catalysts which correspond to residues of the organometallic precursor.

In order to know about what amount of chlorine remains on the catalysts, p2 sample was exposed to chlorine-free water at boiling temperature for several hours. After it, the solid was filtrated and Cl^- in the remaining liquid titrated with $AgNO_3$. The result indicates that after the pretreatment the catalyst retains at least 30% of the initial chlorine [2]. Similar results were obtained for Ru and Ru–Mo catalysts [44,45].

5.2. H_2 chemisorption

Table 2 summarizes the hydrogen chemisorption measurements results. Low chemisorption values in the p2 sample are probably due to the presence of residual chlorine which remains in the catalysts after the treatments. By the way, preparation of catalysts by an organometallic route leads to a rather strong interaction between the metallic phase and the support in the case of low loaded Pd catalysts, this interaction induces structural and/or electronic changes of small palladium crystallites as demonstrated by XPS study [46].

5.3. TPR experiments

TPR profiles of p1 and p2 catalysts are given in Fig. 6, where the hydrogen consumption is plotted against temperature. TPR profiles show a positive peak assigned to the reduction of Pd oxide. The p1 sample showed a peak at 20°C when it was oxidized at 300 and 23°C when it was oxidized at 500°C. On the other hand, the TPR profiles of the p2 catalyst evidence peaks at 35°C for both pretreatments.

For p1 catalysts oxidized at 300°C, the H_2 consumption is almost 90% higher than expected. Characteristic negative peak attributed to palladium hydride decomposition is observed. The small peak correlates well with the average particle size showed by the sample, since the hydride formation is a volumetric phenomena. The extra gas uptake may be attributable to the presence of precursor residues, but this is difficult because the severe calcination treatment during the preparation step and the reported data in the open literature (see Section 5.1). It has been reported [47] that samples with low metal content are able to form oxygen-rich, highly dispersed species, during oxidizing treatments. Hoost and Otto [48]

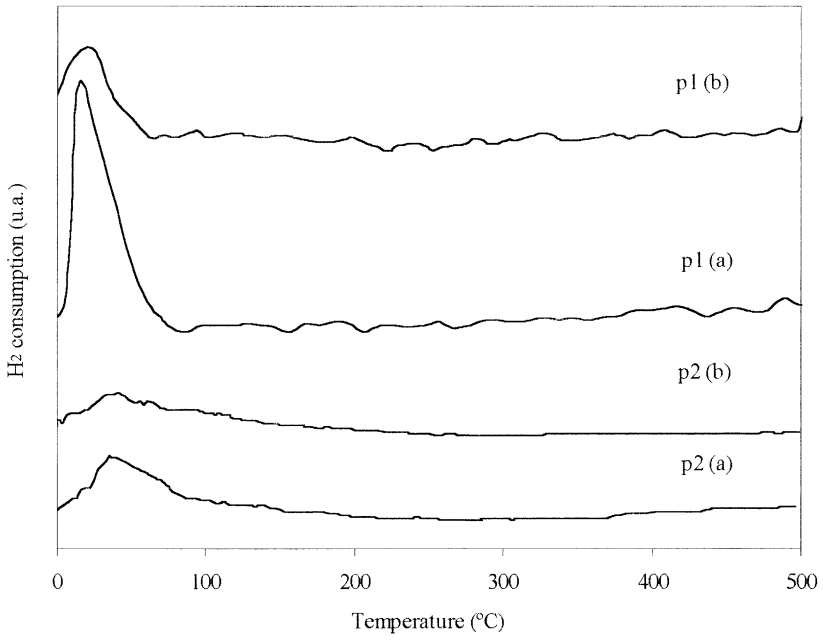

Fig. 6. TPR profiles for p1 and p2 samples. Oxidation temperature: (a) 300°C; (b) 500°C.

reported that on Pd/alumina catalysts with low metal concentrations (<1 wt.% Pd), the oxygen consumed during temperature-programmed oxidation (TPO) was significantly in excess of that expected from O/Pd ratio of one, which suggests the formation of a highly dispersed, oxygen-rich Pd-alumina species. This fact could explain the higher hydrogen consumption in the first TPR. After the exposure to a reductive atmosphere at high temperature (up to 500°C during the TPR) and a new oxidation step at 500°C these small particles could suffer a restructuration or sintering that avoids the oxygen rich species formation.

TPR profiles of p2 sample are brader than profiles of p1. This fact might be associated to the presence of several particle sizes. Negative peak is not observed. Rodríguez Cárdenas [49] reported a double peak of desorption in supported Pd catalysts when the precursor was $PdCl_2$. The author pointed out that the chlorine presence affects the hydride decomposition because it increases the hydride desorption energy, and therefore it requires higher temperature to evolve. The author found that the negative peak corresponding to the Pd normal hydride changes its placement with the particle size. In other words, the hydride decomposes at higher temperature for catalysts with higher dispersion. However, this negative peak assigned to the chlorine effect does not vary with the dispersion. Koopman et al. [50] reported that chlorine stabilizes small Ru particles when Ru catalysts are prepared using $RuCl_3$ hydrated as precursor. Although it is known that small particles do not form hydride, chlorine could extend the hydride formation to smaller particles. Therefore, the final effect would be the combination between the particle size and the hydride stabilization due to the presence of chlorine. Noronha et al. [51] reported that the TPR profile of Pd/Al_2O_3 (Cl) showed a peak at 147°C and a broad desorption peak between 327 and 527°C. On the other hand, the TPR profile of Pd/Al_2O_3 (N) was different. A hydrogen consumption at room temperature was observed, followed by a negative peak around 64°C assigned to the desorption of weakly adsorbed hydrogen from the palladium surface and the decomposition of palladium hydride. They concluded that the Pd oxychloride species are more strongly linked to the support than the PdO species, which explains the reduction at higher temperatures. Thus, the peak at 147°C was assigned to the reduction of PdO_xCl_y whereas the hydrogen consumption at room temperature corresponded to the reduction of PdO. Our results are in qualitative agreement with those of Nyberg and Tengstal [54]. The chlorinated catalysts do not present Pd hydride.

Taking into account that *catalytic activity measurements* indicate a strong interaction metal–halogen, we consider that the negative peak is not observed in sample p2 because it would be overlapped by the consumption peak. Rakai et al. [52] studied the diffuse reflectance spectra of bulk PdO with those of alumina-supported Pd samples prepared from chloride. They reported the presence of chloride ions in the coordination sphere of Pd^{2+} ions which suggests the formation of oxychloride species during calcination in air.

5.4. Catalytic activity measurements

Fig. 7 shows the methane conversion as a function of the temperature of reaction. Since the same metal mass was used in reaction, relative performances can be discussed. For the p1 sample the reaction began at a temperature close to 250°C and the 100% conversion level was attained at 450°C. The p2 sample did not attain the 100% conversion level whatever the temperature. Carbon monoxide formation was never detected in the temperature range studied.

The results of the activity test are shown in Fig. 8. Aged p1 presents a moderate decrease in the activity. This fact might be originated by carbon formation on the active sites when the catalyst was exposed to reaction. The carbon formation may be responsible of the color change of the catalysts after reaction. Aged p2 manifests a better behavior. The activation appears to be associated with chlorine removal. It was reported [3,5–8] that chlorine is a reversible poison and the catalyst activity improves during repeated runs and reductive treatments.

5.5. IR studies

The infrared spectra of p1 and p2 after reaction are given in Fig. 9. Those corresponding to the alumina are also given. In p1 spectrum, two absorption bands were observed, at 2850 and 2950, which are assigned to CH_x species following Gerei et al. [53].

The presence of carbon could be one of the reasons of the color change and the deactivation showed by

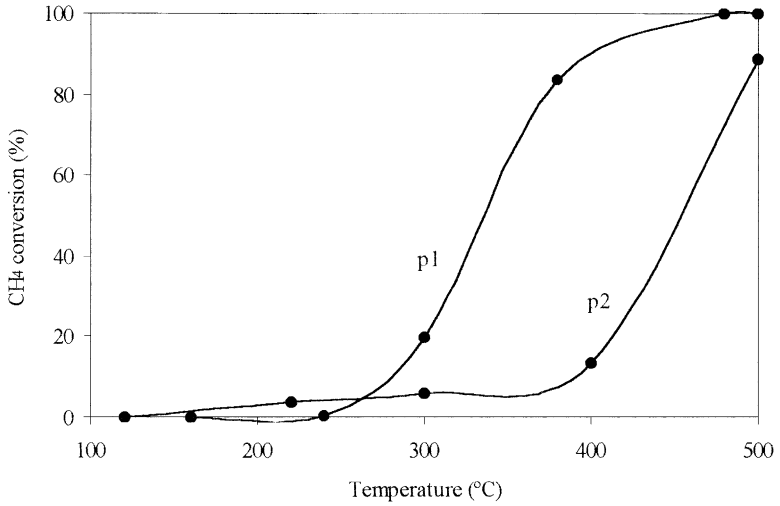

Fig. 7. Methane conversion as a function of reaction temperature.

the aged sample. Pecchi et al. [43] found that carbon deposition occurs upon catalytic reaction on 0.5 wt.% Pd/SiO_2 surface using a reactant mixture containing $1\%CH_4$–$2\%O_2$ in He.

5.6. Theoretical calculations

5.6.1. Oxygen adsorption and dissociation

Analyzing the different situations we found that both positions of O_2 adsorption were possible. Results are summarized in Table 3. The data in Table 3 may only provide a rough qualitative idea of the charge distribution. The minimum O_2-surface distances is obtained in PdO(film)/Pd(0) at 1.9 Å and the longest is for the PdO(film)-Cl/Pd(0) (3.2 Å), in the horizontal position.

Oxygen dissociation on top site (Scheme 7) was favorable in all the considered models (Table 4). The large adsorption energies of O imply that O can be strongly trapped on the surface. This result is in

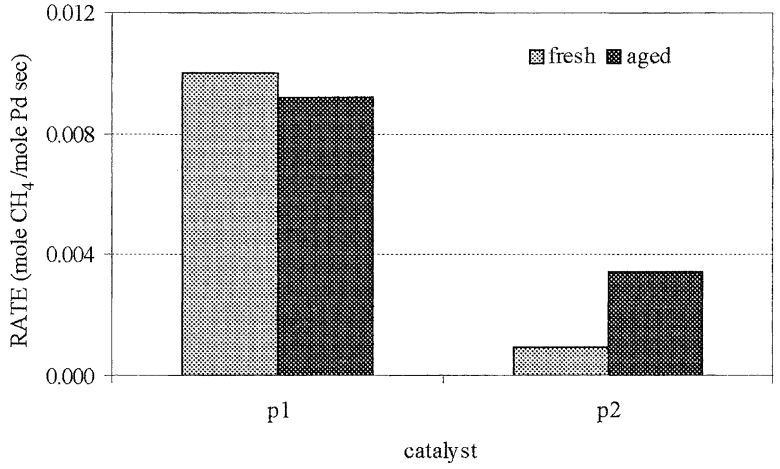

Fig. 8. Methane oxidation rates at 350°C.

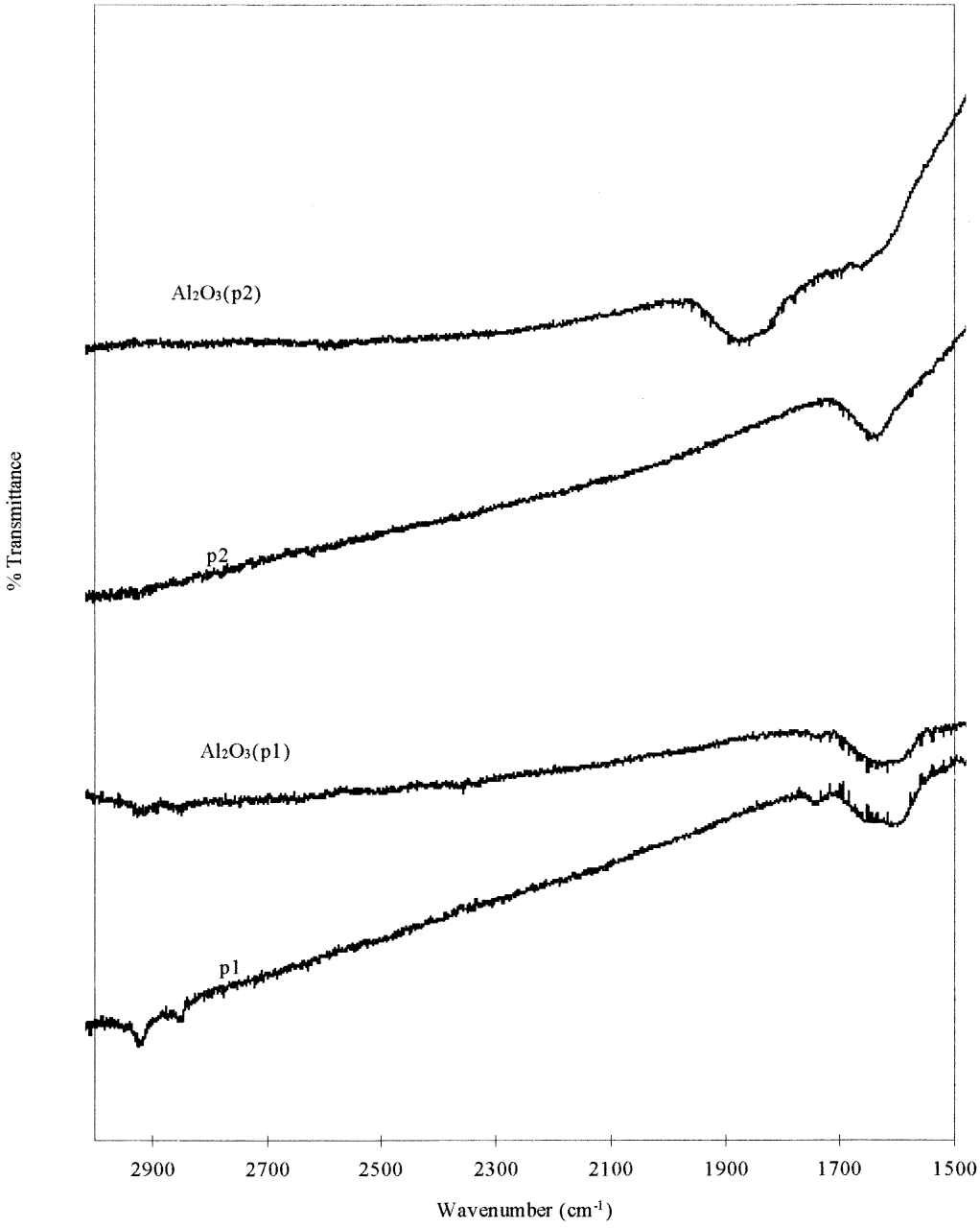

Fig. 9. IR spectra.

agreement with the experimental observations since dissociative adsorption has been reported even at very low temperature on Pd(1 0 0) [54]. The dissociation energy is the most favorable for PdO(film)-Cl/Pd(0) and the least is for PdO(film)/Pd(0). In this case, the distance Pd–O_t is 1.9 for PdO(film)/Pd(0) and very much longer when Cl is present (see Table 4) near 3.1 Å. Cl does not affect dissociation energies in PdO

Table 3
Results for oxygen adsorption

Model	O_2 horizontal		O_2 perpendicular	
	Adsorption energy (eV)	Distance O–Pd (Å)	Adsorption energy (eV)	Distance O–Pd (Å)
Pd(0)	−12.74	2.3	−12.63	3
PdO(cluster)/Pd(0)	−12.67	2.7	−12.62	3.1
PdO(film)/Pd(0)	−12.67	1.9	−12.57	3.1
Pd0(cluster)-Cl/pd(0)	−12.67	3.1	−12.67	3.6
PdO(film)-Cl/Pd(0)	−12.57	3.2	−12.56	3.6

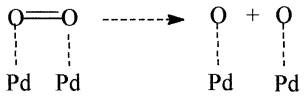

Scheme 7. Model of O_2 dissociation.

Table 4
Results for oxygen dissociation on top site

Model	Dissociation energy (eV)	Distance O–Pd (Å)
Pd(0)	−16.67	2.3
PdO(cluster)/Pd(0)	−17.44	2.7
PdO(film)/Pd(0)	−15.86	1.9
PdO(cluster)-Cl/Pd(0)	−17.7	3.8
PdO(film)-Cl/Pd(0)	−17.9	3.1

cluster/Pd(O), but the O–Pd distance is very much longer (almost 1.1–1.2 Å).

5.6.2. Methane adsorption and dissociation

The results are collected in Tables 5 and 6. The energies involved in the adsorption of C are lower than those for O_2. The on-top sites are more favorable [36]. Form 'a' (Scheme 2) is preferred on models where Pd atoms were not impeded: Pd(0) and PdO(cluster)/Pd(0). Form 'c' is preferred on PdO(film)/Pd(0) and when Cl is present. Form 'b' or 'd' is not so probable. From Table 6 can be concluded that the preferred distance C–Pd or C–O_h is 2.4–2.6 Å for CH_4 adsorption.

Table 5
Calculated adsorption energies (eV) for CH_4 adsorbed on different models

Model	Adsorption energy (eV)			
	a[a]	*b*	*c*	*d*
Pd(0)	−0.94	−0.39	–	–
PdO(cluster)/Pd(0)	−0.86	−0.37	−0.64	−0.24
PdO(film)/Pd(0)	−0.97	−0.4	−1.26	−0.59
PdO(cluster)-Cl/Pd(0)	−0.44	–	−0.56	–
PdO(film)-Cl/Pd(0)	−0.49	–	−0.88	–

[a] Adsorption form according to Scheme 2.

Table 6
Calculated C–X (X: Pd or O) distances (in Å) for CH_4 adsorption

Model	Distance C–X (X: O or Pd) (Å)			
	a[a]	*b*	*c*	*d*
Pd(0)	2.6	2	–	–
PdO(cluster)/Pd(0)	2.6	2.1	2.5	2
PdO(film)/Pd(0)	2.6	2	2.4	1.8
PdO(cluster)-Cl/Pd(0)	3	–	2.6	–
PdO(film)-Cl/Pd(0)	2.9	–	2.6	–

[a] Adsorption form according to Scheme 2.

For the dissociation of CH_4, H was positioned on a Pd, O or Cl atom (Scheme 3). The values in Tables 7 and 8 were obtained optimizing H-surface distance. When CH_3 was bonded to a Pd atom, H was found to prefer a Pd atom on clusters without chlorine. On the other hand, when chlorine was present, dissociation energies were similar in the three options, but smaller (Scheme 3a). When methyl group was positioned on O_h atom, H preferred to adsorb on top of a Pd atom on Cl-free clusters. In models containing chlorine, Pd atoms were impeded, therefore, adsorption on O or Cl atoms was favorable, both with similar energies. The main difference between the surfaces with and without chlorine in CH_4 dissociation is the distance H–X found (all longer than 3.4 Å) whereas when the

Table 7
Calculated dissociation energies (eV) for CH_4 on different models (see Scheme 3)

Model	Dissociation energy (eV)					
	C → Pd, H → X (X: Pd, O or Cl)			C → O, H → X (X: Pd, O or Cl)		
	Pd[a]	O	Cl	Pd	O	Cl
Pd(0)	−3.48	–	–	–	–	–
PdO(cluster)/Pd(0)	−2.8	–	–	−2.6	–	–
PdO(film)/Pd(0)	−2.98	–	–	−2.54	–	–
PdO(cluster)-Cl/Pd(0)	−1.3	−1.2	−1.3	−1.58	−1.58	−1.59
PdO(film)-Cl/Pd(0)	−1.85	−1.76	−1.81	−1.82	−1.8	−1.8

[a] Site of H adsorption.

Table 8
Calculated H–X distances (X: Pd, O or Cl) (in Å) after CH_4 dissociation (see Scheme 3)

Model	Distance H–X (X: O, Pd or Cl) (Å)					
	C → Pd, H → X (X: Pd, O or Cl)			C → Pd, H → X (X: Pd, O or Cl)		
	Pd[a]	O	Cl	Pd	O	Cl
Pd(0)	1.3	–	–	–	–	–
PdO(cluster)/Pd(0)	1.3	–	–	1.3	–	–
PdO(film)/Pd(0)	1.3	–	–	1.3	–	–
PdO(cluster)-Cl/Pd(0)	4.2	5	4.6	6	36	3.9
PdO(film)-Cl/Pd(0)	5	5	4.3	3.4	3.4	3.9

[a] H site of adsorption.

surface is Cl-free, the distances reach values of 1.3–2.0 Å
(see Table 8).

5.6.3. Chlorine loss

Scheme 4 represents removal of chlorine from the catalyst surface. Table 9 summarizes results in terms of relative energy. Form 'b' (Scheme 4) is possible although the energy involved is lower than for 'a'. From our results it can be concluded that if H is adsorbed on Cl near to Pd–CH_3 is easier to remove it than if it is near CH_3–O_h.

Table 9
Calculated energies (eV) for removal of chlorine from the catalyst surface during methane combustion

Model	Relative energy (eV)	
	a[a]	*b*
PdO(cluster)-Cl/Pd(0)	−0.49	0.11
PdO(film)-Cl/Pd(0)	−0.5	−0.03

[a] Reaction according to Scheme 4, distance H–Cl = 1.2746 Å.

5.6.4. Water adsorption

The results of EHMO calculations on this topic are given in Table 10. Our results seem to indicate that there is no difference between the different surfaces in terms of water adsorption. Water desorption from O_h surface and oxygen vacancy formation was energetically favorable (−0.4 eV) for PdO(film)/Pd(O), where it is more probable the water formation.

LEED patterns suggest that on fcc (1 1 1) and hcp (0 0 0 1) surfaces, O atoms are adsorbed in the three-fold hollow sites, while for H_2O, theoretical

Table 10
Calculated adsorption energies (eV) and O–Pd heights (in Å) for H_2O on different models

Model	Adsorption energy (eV)	Distance O–Pd (Å)
PdO(cluster)/Pd(0)	−0.65	2.6
PdO(film)/Pd(0)	−0.63	2.6
PdO(cluster)-Cl/Pd(0)	−0.62	2.7
PdO(film)-Cl/Pd(0)	−0.61	2.8

Table 11
Calculated adsorption energies (eV) for CO_2 on different models

Model	Adsorption energy (eV)				
	a[a]	*b*	*c*	*d*	*e*
PdO(cluster)/Pd(0)	−13.97	−11.4	−0.09	−2.55	−0.66
PdO(film)/Pd(0)	−14.78	−11.29	−0.09	−2.00	−1.23
PdO(cluster)-Cl/Pd(0)	−10.35	−11.10	−0.06	−0.76	−0.23
PdO(film)-Cl/Pd(0)	−10.4	−12.2	−0.04	−0.43	−0.41

[a] Adsorption form according to Scheme 5.

Table 12
Calculated heights (in Å) for CO_2 adsorption on different models

Model	Distance C– (O or Pd) (Å)				
	a[a]	*b*	*c*	*d*	*e*
PdO(cluster)/Pd(0)	1.6	3.5	2.6	2.1	2.2
PdO(film)/Pd(0)	1.7	3.5	2.6	2.1	2.2
PdO(cluster)-Cl/Pd(0)	1.8	4	2.8	2.6	2.7
PdO(film)-Cl/Pd(0)	4	3.5	2.9	2.8	2.7

[a] Adsorption form according to Scheme 5.

calculations indicate the top adsorption on the metal atoms as the most stable (see in [55]). There are data about the behavior of water on oxygen-precovered surfaces; the presence of O atoms on Pd (1 0 0) causes high-temperature H_2O desorption [56,57].

5.6.5. Carbon dioxide adsorption

Adsorption energies are collected in Tables 11 and 12. Adsorption of carboxylate form was more favorable in all models. It agrees with literature data about interaction of CO_2 with several oxides like Co_3O_4 [38], NiO [39], CuO and Cu_2O [58], CuO–$CuCr_2O_4$ [59], La_2O_3 and $La(OH)_3$ [60]. In those cases, where the CO_2 species took place on the Cl-containing surfaces, the total energy of adsorbed species is smaller. The adsorption energy of CO_2 is higher for PdO(film)/Pd(0) (form 'a') whereas is lower for PdO(cluster)/Pd(0). When chlorine is present, form 'b' on PdO(film)/Pd(0) is preferred.

Forms 'a' and 'b' are preferred. It can be seen again that the chlorine makes the distances C–O_h or Pd much longer (1.6–1.7 Å versus 3.5–4.0 Å).

5.6.6. Steps of product desorption — reactive adsorption–dissociation on two possible reaction mechanisms

The Scheme 6 shows the evaluated situations for both mechanisms. Tables 13 and 14 collected

Table 13
Relative energies (eV) for steps of products desorption — reactive adsorption in surface reaction (Langmuir–Hinshelwood)

Model	C → Pd, H → X (X: Pd or Cl)[a]		C → O, H → X (X: Pd or Cl)[b]	
	Pd	Cl	Pd	Cl
PdO(cluster)/Pd(0)	−47.69	–	−49.67	–
PdO(film)/Pd(0)	−44.91	–	−34.67	–
PdO(cluster)-Cl/Pd(0)	−48.74	−48.64	−37.37	−31.93
PdO(film)-Cl/Pd(0)	−35.34	−35.24	−33.62	−32.81

[a] According to Scheme 6(2).
[b] According to Scheme 6(1).

Table 14
Relative energies (eV) for steps of products desorption — reactive adsorption in surface reaction (Mars and van Krevelen)

Model	C → Pd, H → X (X: Pd or Cl)[a]		C → O, H → X (X: Pd or Cl)[b]	
	Pd	Cl	Pd	Cl
PdO(cluster)/Pd(0)	−39.91	–	−43.11	–
PdO(film)/Pd(0)	−34.99	–	−30.54	–
PdO(cluster)-Cl/Pd(0)	−37.06	−37.14	−33.91	−37.74
PdO(film)-Cl/Pd(0)	−32.62	−32.59	−32.81	−25.51

[a] According to Scheme 6(2).
[b] According to Scheme 6(1).

the results. Both mechanisms are probable but normal surface reaction (L–H) is preferred. On PdO(cluster)/Pd(0), the reaction is favored if CH_3 is placed on O atom, but on PdO(film)/Pd(0) it must be on Pd. It is evident that Cl affects the reaction when is present in the film (almost +10 eV in energy).

For Mars and van Krevelen mechanism, again chlorine affect it, but in lesser extension (near +3 eV in energy).

6. Discussion and conclusions

This general discussion must take into account different aspects of the published literature when we want to compare it with our results:

1. The wide range of composition of the reactive mixture [61,62]. Generally an excess of O_2 is used.
2. The different preparation methods, precursors and supports [63–65] used.
3. The pretreatments used in the preactivation step [66].

The catalyst prepared without chlorine had the greatest activity. Early experiments showed that free-Cl catalysts produced notably better activity than catalysts with chlorine. Simone et al. [3] found a correlation between enhanced activity and low chlorine concentration. In a sample with chlorine, the activity improves during reaction. This result agrees with these from Cant et al. [6]. Aged p1 presents a slight decrease in the activity. This fact might be originated by carbon formation on the active sites when the catalyst was exposed to methane oxidation reaction. It is confirmed from IR results and color change after reaction. Carbonaceous compounds were reported when stoichiometric reactant mixture is used [43]. Generally carbon is not observed because oxidant mixtures are used. Haack and Otto [67] reported structure-sensitivity in supported Pd catalysts suggested by a change in carbon deposition derived from incomplete methane oxidation. Normalized to Pd, the intensity of the carbon deposit decreases with increasing Pd particle sizes. Carbon deposits are substantial for highly dispersed Pd on alumina for all supported samples with substoichiometric and stoichiometric reactant mixture.

Our TPR and chemisorption measurements results indicate that different precursors and/or preparation methods generate different metallic particles.

Our results of EHMO calculations show that increasing the amount of O on the catalyst, the methane oxidation reaction is not so favored. The key points seem to be the methane dissociation, CO_2 adsorption energy and the step of desorption of products, adsorption–dissociation of reactives. Tables 13 and 14 show how the energy increases when the surface is partially covered with oxygen.

The Pd–O distances found when O_2 is adsorbed and dissociated (Table 4) when no Cl is present (1.9 Å) could be assigned to Pd=O. This possibility would be ruled out when O_2 is dissociated near a Cl–Pd bond (Pd–O distance 3.1 Å). This fact could be related to the C formation when no chlorine is present because the Pd=O bond is stronger.

These results agree with part of literature. Cullis and Willatt [63] reported that Pd/γ-Al_2O_3 pretreated in a hydrogen–helium mixture were most

readily activated but those pretreated with oxygen had a very low activity. Similar results were found for Müller et al. [68] and Pecchi et al. [43]. Oh et al. [69] suggested that oxygen inhibits the methane oxidation because oxygen migrates into the bulk of the palladium, forming unreactive bulk palladium oxide. They conclude that oxygen blocks the methane oxidation by excluding the adsorption of methane at active sites. Carstens et al. [70] observed that methane combustion activity of PdO can be enhanced by producing a small amount of metallic Pd on the surface of PdO. The metallic Pd is more effective than PdO for the dissociative adsorption of methane.

Contradictory information exits about CO_2 effects in methane oxidation. Cullis et al. [71] found little inhibition whereas Ribeiro et al. [72] found a strong inhibition above 0.5% volume CO_2. Müller et al. [68] reported that adsorption of CO_2 occurs to a much larger extent than the adsorption of O_2 and H_2O on Pd/Zr with stoichiometric mixture. Our results agree with the last work (see Table 11).

The adsorption energies for CH_4 are only slightly more negative than for H_2O. In this sense water is an inhibitor of the CH_4 adsorption and the possibility of $Pd(OH)_x$ formation cannot be ruled out. Water is well known to inhibit methane oxidation over palladium catalysts [31,63,71,73].

Our results of EHMO calculations would indicate Langmuir–Hinshelwood and Mars and van Krevelen mechanisms are probable, with similar energies. It agrees with Müller et al. [68], who found that in methane combustion at least 20% of CO_2 is formed from a redox reaction, whereas the remaining amount may be produced via normal surface reaction between adsorbed carbon containing species and oxygen.

The carbon formation is a proposed explanation for the decrease of activity. The possibility of stronger dehydrogenat ion cannot be ruled out in Pd, especially if O_2 is at low concentrations. If O_2 is not adsorbed in the neighborhood of CH_4, the CH_3–Pd form can be further dehydrated. In this sense the result of dissociation of CH_4 on Pd is very useful (see Table 6). This situation occurs when an stoichiometric amount of O is used. Probably with excess oxygen this effect is not acting (see Fig. 8). When chlorine was present, energies of CH_4 dissociation are smaller and when chlorine is loosing (as HCl), anion vacancies are formed on the surface and they favor oxygen adsorption. Both situations lead to prevent carbon formation and it coincides with IR spectra and the change of color in p1 before and after the reaction. Several explanations could be applied to the color change in p1. An alternative one to the presented above would be the possibility of the occurrence of Mars and van Krevelen mechanism, especially because we used stoichoimetric mixture with low O content (2%). In this case, the water loss because reaction between H from methane dissociation and O from oxidized surface is a possibility. Results of EHMO calculation demonstrate that this reaction path is possible ($E = -0.4\,\text{eV}$). Therefore, a combined effect could be the cause of the color change: carbon formation and partial Pd reduction because Mars and van Krevelen mechanism.

The profiles showed in Fig. 7 are easy to understand seeing the energies for chlorine loss (near $-0.5\,\text{eV}$). Higher temperatures are needed to avoid the undesirable effect of chlorine (blocking of adsorption sites for O_2 and CH_4 adsorption and dissociation).

Residual amounts of chlorine do not affect the adsorption of water but the desorption energy of CO_2 is not negative. Adsorption and dissociation of CH_4 are difficulted by Cl, but desorption of CO_2 is favored when Cl is present because lower adsorption energies of it (see Table 11). The net effect would be the increasing of conversion with temperature at temperatures higher than 400°C, when chlorine is lost. The chlorine loss would have two effects: amounts of carbon formed initially because CH_4 dissociation and later oxidation of this C with O_2 from the mixture. The strongly bonded chlorine would be responsible of the lower conversion in this catalyst.

After ageing, the combined effects of chlorine loss and surface oxidation would increase the conversion as we can see in Fig. 8.

Acknowledgements

We are grateful to Professor Alfredo Juan of Universidad Nacional del Sur, Departamento de Física, for providing the modified version of ICONC and for he1pful advice. We thank the Universidad Nacional del Sur (UNS) and the Consejo Nacional de investigaciones Cientificas y Técnicas (CONICET) for their financial support.

References

[1] R. Hicks, H. Qi, M. Young, R. Lee, J. Catal. 122 (1990) 295.
[2] L. Konopny, A. Juan, D. Damiani, Appl. Catal. B 15 (1998) 115.
[3] D. Simone, T. Kenneily, N. Brungard, R. Farrauto, Appl. Catal. 70 (1991) 87.
[4] Y. Shen, L. Cai, J. Li, S. Wang, K. Huang, Catal. Today 6 (1989) 47.
[5] P. Marecot, A. Fakche, B. Kellali, G. Mabilon, M. Prigent, J. Barbier, Appl. Catal. B 3 (1994) 283.
[6] N. Cant, D. Angove, M. Patterson, Catal. Today 44 (1998) 93.
[7] C. Cullis, B. Willatt, J. Catal. 86 (1984) 187.
[8] H. Lieske, G. Lietz, H. Spendler, J. Volter, J. Catal. 81 (1983) 8.
[9] J. Barbier, D. Bahloul, P, Marecot, J. Catal. Lett. 8 (1991) 327.
[10] E. Marceau, M. Che, J. Saint-Just, J. Tatibouet, Catal. Today 29 (1996) 415.
[11] S. Peri, C. Lund, J. Catal. 152 (1995) 410.
[12] H. Rodríguez Cárdenas, D. Damiani, in: C.H. Bartholomew, J.B. Butt (Eds.), Catalyst Deactivation, Elsevier, Amsterdam, 1991, p. 667.
[13] J. Stencel, G. Goodman, B. Davis, in: M.J. Phillips, M. Ternan (Eds.), Proceedings of the 9th International Congress on Catalysis, Vol. 3, Calgary, 1988, Chemical Institute of Canada, Ottawa, p. 1291.
[14] H. Miur, H. Hondou, K. Sugiyama, T. Matsuda, L. Gonzalez, in: M.J. Phillips, M. Ternan (Eds.), Proceedings of the 9th International Congress on Catalysis, Vol. 3, Calgary, 1988, Chemical Institute of Canada, Ottawa, p. 1291.
[15] J. Anderson, Structure of Metallic Catalysts, Academic Press, New York, 1975, p. 296.
[16] S. Robertson, B. Mc Nicol, J. de Baas, S. Kloet, J. Jenkins, J. Catal. 37 (1975) 424.
[17] D. Damiani, E. Pérz Millán, A. Rouco, J. Catal. 101 (1986) 162.
[18] R. Hoffmann, J. Chem. Phys. 39 (6) (1963) 1397.
[19] R. Sumerville, R. Hoffmann, J. Am. Chem. Soc. 98 (1976) 23.
[20] P. Hay, J. Thibeault, R. Hoffmann, J. Am. Chem. Soc. 97 (1975) 4884.
[21] I. Chamber, L. Forrs, G. Calzaferri, J. Phys. Chem. 93 (1989) 5366.
[22] A. Anderson, R. Hoffmann, J. Chem. Phys. 60 (1974) 4271.
[23] W. Lotz, J. Opt. Soc. Am. 60 (1970) 206.
[24] A. Vela, L. Gázquez, J. Phys. Chem. 92 (1985) 5366.
[25] I. Chamber, L. Forrs, G. Calzaferri, J. Phys. Chem. 93 (1989) 5366.
[26] M. Ferreira, N. Castellani, D. Damiani, A. Juan, J. Mol. Catal. A: Chem. 122 (1997) 25.
[27] M. Ferreira, D. Damiani, A. Juan, Comput. Mater. Sci. 9 (1998) 357.
[28] R. Hicks, H. Qi, M. Young, R. Lee, J. Catal. 122 (1990) 280.
[29] P. Briot, M. Primet, Appl. Catal. 68 (1991) 301.
[30] E. Garbowsky, C. Feumi-Jantou, N. Mouaddib, M. Primet, Appl. Catal. A 109 (1994) 277.
[31] F. Ribeiro, M. Chow, R. Dalla Betta, J. Catal. 146 (1994) 277.
[32] C. Cullis, B. Willat, J. Catal. 83 (1983) 267.
[33] T. Ward, P. Alemany, R. Hoffmann, J. Phys. Chem. 97 (29) (1993) 7691.
[34] A. Rochefort, J. Andzelm, N. Russo, D. Salahub, J. Am. Chem. Soc. 112 (23) 1990.
[35] A.F. Wells, Structural Inorganic Chemistry, 5th Edition, Oxford Science Publications, Oxford, 1986.
[36] C.-T. Au, C.-F. Ng, M.-S. Liao, J. Catal. 185 (1999) 12.
[37] M. Levan, A. Hubbard, J. Electroanal. Chem. 74 (1976) 253.
[38] D. Klissrski, J. Catal. 33 (1974) 149.
[39] A. Ueno, J. Hochmuth, C. Bennett, J. Catal. 49 (1977) 225.
[40] E. Lesage-Rosenberg, G. Vlaic, H. Dexpert, P. Legarde, E. Freund, Appl. Catal. 22 (1986) 21.
[41] D. Lomot, W. Juszcyk, Z. Karpinsid, F. Bozon-Verduraz, New J. Chem. 21 (1997) 977.
[42] D. Lomot, W. Juszcyk, Z. Karpinski, F. Bozon-Verduraz, J. Chem. Soc., Faraday Trans. 93 (10) (1997) 2015.
[43] G. Pecchi, P. Reyes, I. Concha, J. Fierro, J. Catal. 179 (1998) 309.
[44] G.C. Bond, R.R. Rajaram, R. Burch, Appl. Catal. 27 (1986) 379.
[45] A. Juan, D. Damiani, J. Catal. 137 (1992) 77.
[46] J. Goetz, M. Volpe, A. Sica, C. Gigola, R. Touroude, J. Catal. 153 (1995) 86.
[47] A. Pisanu, Thesis, U.N.S, 1998.
[48] T. Hoost, K. Otto, Appl. Catal. A 92 (1992) 39.
[49] H. Rodriguez Cárdenas, Thesis, U.N.S., 1987.
[50] P. Koopman, A. Kieboom, H. Van Bekkum, J. Catal. 69 (1981) 172.
[51] F. Noronha, M. Baldanza, M. Schmal, J. Catal. 188 (1999) 270.
[52] A. Rakai, D. Tessier, F. Bozon-Verduraz, New J. Chem. 16 (1992) 86.
[53] S. Gerei, E. Rozhkova, Y. Gorokhovatsky, J. Catal. 28 (1973) 341.
[54] C. Nyberg, C. Tengstal, Surf. Sci. 126 (1983) 163.
[55] J. Heras, L. Viscido, Catal. Rev. Sci. Eng. 30 (2) (1988) 281.
[56] E. Stuve, S. Jorgensen, R. Madix, Surf. Sci. 146 (1984) 179.
[57] C. Nyberg, C. Tengstal, J. Chem. Phys. 80 (1984) 3463.
[58] S. Gerei, E. Rozhkova, Y. Gorokhovatsky, J. Catal. 28 (1973) 341.
[59] W. Herti, R. Farrauto, J. Catal. 29 (1973) 352.
[60] M. Rosynek, D. Magnuson, J. Catal. 48 (1977) 417.
[61] D. Konig, W. Weber, D. Poindexter, J. McBride, G. Graham, K. Otto, Catal. Lett. 29 (1994) 329.
[62] N. Mouaddib, C. Feumi-Jantou, E. Garbowski, M. Primet, Appl. Catal. A 87 (1992) 129.
[63] C. Cullis, B. Willatt, J. Catal. 83 (1983) 267.
[64] Y. Yazawa, H. Yoshida, N. Takagi, S. Komai, A. Satsuma, T. Hattori, J. Catal. 187 (1999) 15.
[65] K. Muto, N. Katada, M. Niwa, Appl. Catal. A 134 (1996) 203.
[66] M. Lyubovsky, L. Pferfferle, Appl. Catal. A 173 (1998) 107.

[67] L. Haack, K. Otto, Catal. Lett. 34 (1995) 31.
[68] C. Müller, M. Maciejewski, R. Koeppel, A. Baiker, Catal. Today 47 (1999) 245.
[69] S. Oh, P. Mitchell, R. Siewert, J. Catal. 132 (1991) 287.
[70] J. Carstens, S. Su, A. Bell, J. Catal. 176 (1998) 136.
[71] C. Cullis, T. Nevell, D. Trimm, J. Chem. Soc., Faraday Trans. 1 68 (1972) 1406.
[72] F. Ribeiro, M. Chow, A. Dalla Betta, J. Catal. 146 (1994) 537.
[73] R. Burch, P. Loader, F. Urbano, Catal. Today 27 (1996) 243.